Facile and eco-friendly fabrication of Cu_2O truncated octahedral crystallites with enhanced antibacterial performance against *Escherichia coli* and *Staphylococcus aureus*

Chunmei Yang, Qing Li ✉, *Hua Lin, Yuan Li, Guomeng Xie*

Faculty of Materials and Energy, Southwest University, Chongqing 400715, People's Republic of China
✉ *E-mail: qli@swu.edu.cn*

Published in Micro & Nano Letters; Received on 18th December 2015; Revised on 3rd April 2016; Accepted on 7th April 2016

Truncated octahedral cuprous oxide (Cu_2O) crystallites with highly uniform morphologies and sizes ranging from 2.4–2.5 μm were prepared by using a green and convenient approach and their antibacterial activities were studied. They were obtained through the chemical reduction of copper chloride by glucose in the presence of sodium hydroxide and polyethylene glycol at room temperature for 2 h. X-ray powder diffraction, energy dispersive spectrometer, scanning electron microscopy, and transmission electron microscopy as well as high-resolution transmission electron microscopy (HRTEM) were used to characterise the obtained products. Structural analysis revealed that these truncated octahedral crystallites were composed of eight {111} faces and six {200} faces. The effects of time, temperature and polyethylene glycol on the formation of truncated octahedral cuprous oxide were investigated. The possible growth process and mechanism of truncated octahedral cuprous oxide were proposed. The antibacterial activities of truncated octahedral Cu_2O were also explored. They exhibited significant antimicrobial activity against both gram-negative and gram-positive bacteria. The result of antibacterial study revealed that the prepared Cu_2O can be a promising candidate for wide range of bio-medical applications.

1. Introduction: Micro-nanomaterials have received more and more interests from scientists. The physical and chemical properties of micro-nanomaterials such as surface plasmon resonance frequency [1], band gap [2], magnetic properties [3] and the total surface area [4] depend on their sizes and shapes. The regular micro-nanostructure has extensive applications in the fields of photons, nanoelectronics, catalysis, information storage and biosensor [5].

Cu_2O is a p-type semiconductor with a direct band gap (~2.17 eV) located in the visible range [6]. The intrinsic properties of Cu_2O, such as non-toxic, low price, and good environmental acceptability [7], make it have great potential for industry, which have caused widespread concern in the sterilisation [8], gas sensing [9], electrode for lithium-ion batteries [10], solar energy conversion [11], magnetic storage [12], photochemical evolution of H_2 from water [13] etc. The morphology plays a critical role in these properties. There are some methods for the preparation of cuprous oxide with different shapes. Recently, Huang *et al*. prepared Cu_2O cubic using a seed-mediated synthesis approach in aqueous solution [14], Yue *et al*. [15] synthesised Cu_2O nanowires through thermal stress-induced method. Liang *et al*. [16] have synthesised rhombic dodecahedral Cu_2O microcrystals at 60°C. Currently, the preparation of truncated octahedral Cu_2O is still a challenge at room temperature. Some preparation methods used toxic materials or complex instrument, increasing the environmental burden or the cost and restricting its industrial application. Therefore, there is a desirable approach to develop a green, convenient and low-cost synthetic route to prepare truncated octahedral cuprous oxide microstructures. As common antibacterial material, the industrial application of Ag has been restricted due to its high cost. Therefore, the low-cost Cu_2O has a potential antimicrobial material in bio-medical engineering filed.

In this communication, a green and facile method was used to prepare truncated octahedral Cu_2O at room temperature. The influences of the reaction time, temperature and polyethylene glycol on crystal growth mechanism were discussed. Finally, we studied the antibacterial activities of the obtained truncated octahedral Cu_2O against gram-negative and gram-positive bacteria.

2. Experimental: Copper (II) chloride ($M = 170.48, \geq 99\%$), D-glucose ($M = 198.7$), polyethylene glycol, ethanol ($M = 46.07, \geq 99.7\%$), sodium hydroxide ($M = 40, \geq 96\%$) were used as received. All the chemicals were analytical grade reagents used without further purification. Deionised water was used in the experiment.

The cuprous oxide was prepared through the chemical reduction of copper chloride by D-glucose in the presence of sodium hydroxide. The preparation process of truncated octahedral cuprous oxide was illustrated in Fig. 1. Solution 1 included 10 ml water and 3 ml ethanol. 0.3 g $CuCl_2$ was added to Solution 1 to obtain Solution A. 0.35 g NaOH, 0.31 g $C_6H_{12}O_6$ and 0.12 g polyethylene glycol were added to Solution 1 to get Solution B. Then Solution A and Solution B were mixed into a beaker at room temperature. The pH of mixed solution was 12. Initially, the mixed solution was clear blue. Several minutes later, the reaction system gradually became yellow green, yellow and finally brick red. The reaction was kept stationary for 2 h at room temperature and the final pH was 12. D-glucose reduced Cu^{2+} ions to Cu_2O quickly in the presence of OH^- ions. The resulting brick red precipitate was collected by centrifugation and washed with absolute ethanol and de-ionised water in an ultrasonic cleaning device. All reactions were performed at room temperature. Finally, the precipitate was dried at 50°C for 12 h. The yield of Cu_2O could reach 96% under the optimal reaction condition.

The prepared cuprous oxide was characterised by X-ray powder diffraction (XRD) on a X-ray diffractometer (XD3 system, Beijing Purkinje General Instrument Co., Ltd.) with Cu Kα radiation ($\lambda = 0.154178$ nm) at a scanning rate of $0.02°s^{-1}$ in the 2θ range from 5° to 80°. The scanning electron microscopy (SEM) and energy dispersive spectrometer (EDS) were measured with a FEI Quanta 250 emission SEM equipped with an energy spectrum analytical system. The transmission electron microscopy (TEM), including high-resolution transmission electron microscopy (HRTEM) image and the selected area electron diffraction (SAED) spectrum were taken on a JEM-2100 transmission electron microscope operated at an accelerating voltage of 200 kV with the samples on copper grid.

To explore the potential of truncated octahedral Cu_2O as an antibacterial agent, the bacteriostatic activities of as-prepared truncated

doi: 10.1049/mnl.2015.0512

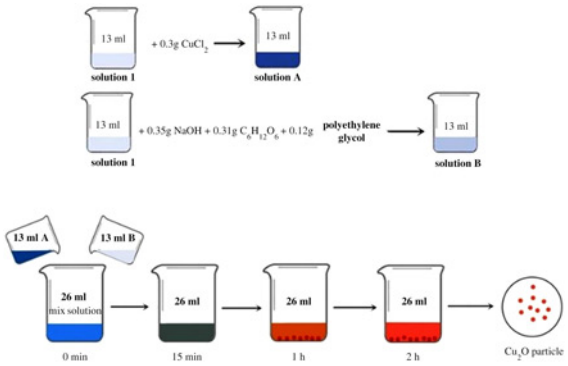

Fig. 1 *Preparation procedure of truncated octahedral Cu_2O*

octahedral Cu_2O were studied against *Escherichia coli* (gram-negative bacteria) and and *Staphylococcus aureus* (gram-positive bacteria). Both as-prepared broth culture medium and agar culture medium were disinfected. *E. coli* and *S. aureus* were inoculated into the culture medium and incubated at 37°C for 24 h. Then *E. coli* and *S. aureus* were diluted with sterilised saline. The 200 µl bacterial liquid and 200 µl different concentrations of Cu_2O samples were mixed in sterile 96-well plates, and the wells without Cu_2O sample were used as the control. Then, the 96-well plates were transferred into an incubator and incubated at 37°C for 16 h. Finally, the concentrations of the remaining strains were measured by a Bio-Tek Biorobot3000 ELISA (enzyme linked immunosorbent assay).

3. Results and discussion: The chemical reaction involved in this work is represented by the following equation. In this experiment, D-glucose, working as a reducing agent, reduced $CuCl_2$ to Cu_2O in the mixture containing polyethylene glycol and NaOH-ethanol aqueous solution. Detailed reaction process is shown in Fig. 2.

$$2Cu^{2+} + C_6H_{12}O_6 + 4OH^- \rightarrow Cu_2O\downarrow + 2H_2O + C_6H_{12}O_7$$

The crystalline phase structure and the purity of the products obtained in the aqueous alcohol at 25°C for 2 h were examined by XRD. The XRD pattern of the cuprous oxide particles was shown in Fig. 3. The five diffraction peaks were observed at 2θ values 29.647°, 36.521°, 42.423°, 61.552° and 73.739°, which corresponded to (110), (111), (200), (220) and (311) planes of face-centred cubic structure of Cu_2O, with dominant sheet growth of the Cu_2O {111} planes. All of the diffraction peaks could be assigned to cubic structure Cu_2O (JCPDS Card No. 05-0667) with the lattice parameter $a = 4.258$ Å, $b = 4.258$ Å, $c = 4.258$ Å. No impurity was observed.

The SEM images of truncated octahedral cuprous oxide were shown in Fig. 4*a*. It was a representative low magnification SEM image of the collected product. From the analysis by using SEM technique, it was found that the particles were uniform and well dispersed truncated octahedron with the average size of 2.5 µm. The crystal structure of truncated octahedral Cu_2O was shown in

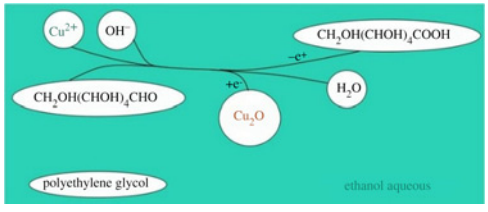

Fig. 2 *Ionic reaction process of Cu_2O synthesis*

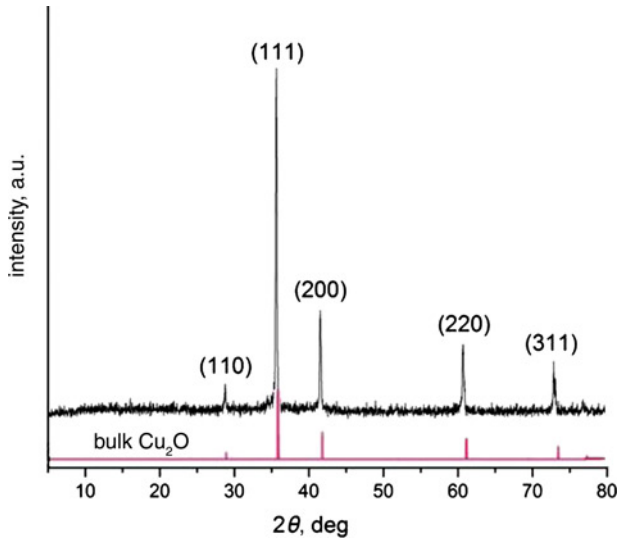

Fig. 3 *XRD pattern of the sample synthesised in the aqueous alcohol at 25 °C for 2 h*

Fig. 5*a*. The red sphere is Cu atom and the yellow is O. The section diagram of the atomic configuration of (111) surface of Cu_2O was shown in Fig. 5*b*. A rectangular unit cell (Fig. 5*b*) with the lattice parameters of $a = 6.021$ Å, $b = 6.021$ Å can be identified in the image, which is consistent with the lattice structure of Cu_2O (111) surface. The truncated octahedral crystallite was composed of eight {111} surfaces and six {200} surfaces (Fig. 5*c*). The morphology of crystal, external reflection of its internal structure, was determined by the relative growth rate of each crystal plane. As the reaction proceeded, the truncated octahedral particles grew along different directions with different growth rates due to their different surface energies. According to the principle of Gibbs–Wullf, the surface energy (γ) of face-centred cubic varies with different lattice plane, whose sequence is $\gamma\{111\} < \gamma\{200\} < \gamma\{110\}$ [17]. Based on the thermodynamic principle, the crystal plane with low specific surface energy, is easily to be exposed on the surface, leading to low growth rate [18]. Hence {111} planes and {200} planes were eventually preserved. The product ultimately grew into truncated octahedral along the (111) and (200) crystal plane. The truncated octahedral Cu_2O was comprised of eight (111) planes and six {200} planes (Fig. 5*c*). The element composition of product spectrum was further checked with EDS. The corresponding EDS spectrum of Cu_2O was shown in Fig. 4*b*. It can be obviously seen that the product contained only Cu and O signals. The C signal coming from environment was unavoidable. The EDS of product were consistent with the XRD result. It further demonstrated that the products were pure cuprous oxide.

Fig. 6*a* was the TEM image of the truncated octahedral Cu_2O. It was obvious that the shape and size of the truncated octahedral

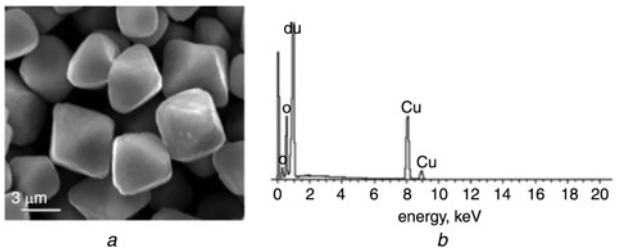

Fig. 4 *SEM images of truncated octahedral cuprous oxide*
a SEM image of the as-obtained Cu_2O
b Corresponding EDS spectrum

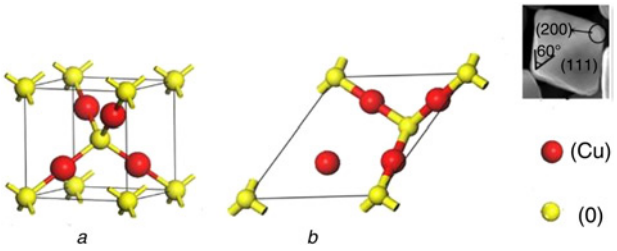

Fig. 5 *Crystal structure of truncated octahedral Cu_2O and atomic configuration*
a Crystal structure of Cu_2O
b Section diagram of the atomic configuration of Cu_2O (111) surface and (200) surface

Cu_2O were conformed to the image of SEM. The crystal orientation and crystallinity of truncated octahedral Cu_2O were further studied with selected area electron diffraction (SAED) methods. Fig. 6*b* was the SAED patterns of the products. The reflections of (110), (111), (200), (220), and (311) planes were obviously seen. The products of truncated octahedral Cu_2O were polycrystalline. The HRTEM image of truncated octahedral cuprous oxide was shown in Fig. 6*c*. The lattice fringes of (200) plane (0.213 nm) were clearly seen, indicating the products were of good crystallinity.

To make out the role of polyethylene glycol, a sample without adding polyethylene glycol was prepared without changing other parameters. The appearance and size of products were highly non-uniform. The above experiments illustrated that polyethylene glycol made the reaction conduct more thoroughly, which may because polyethylene glycol with high dispersity and well adhesion controlled the diffusion rate of the Cu_2O crystal nucleus [19]. Obviously, polyethylene glycol was crucial to the morphologies of the resulting products.

To discuss the growth mechanism of truncated octahedral Cu_2O, the effect of time was explored. A series of time-dependent

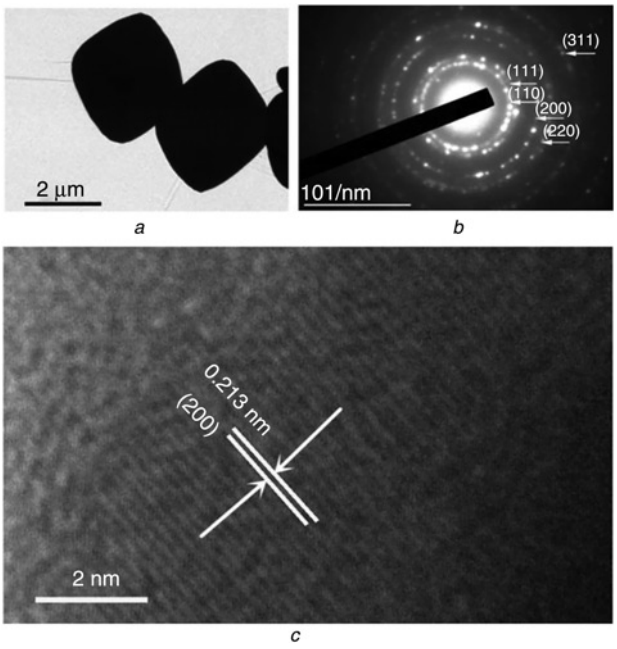

Fig. 6 *TEM image of the truncated octahedral Cu_2O and corresponding electron diffraction pattern*
a TEM images of the truncated octahedral cuprous oxide
b Corresponding electron diffraction pattern
c HRTEM image obtained from the edge of an individual truncated octahedral Cu_2O

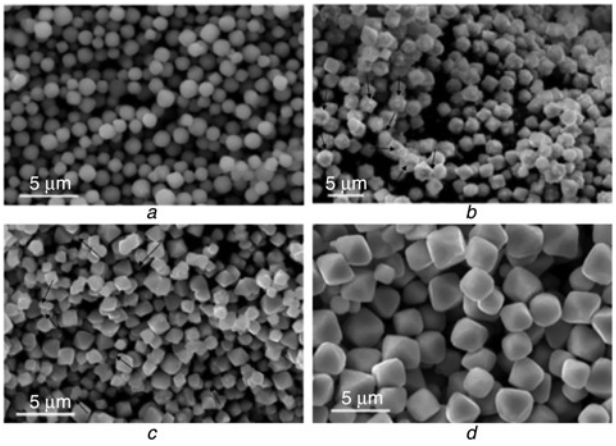

Fig. 7 *SEM images of products with the different reaction time*
a 10 min
b 30 min
c 1 h
d 2 h. Arrows: the exact places of the convex or small particles

experiments were carried out by intercepting intermediate products in different reaction stages of 10 min, 30 min, 1 h and 2 h. Fig. 7 clearly indicated the evolution process of the Cu_2O crystallite by varying the reaction time. First, when Solution A ($CuCl_2$) mixed with Solution B (NaOH, D-glucose, polyethylene glycol), the mixture was translucent. 10 min later, the mixture turned into turbid and the colour became celadon. It indicted that something was created and the reaction began. It can clearly be seen that it directly formed spheroidal Cu_2O (Fig. 7*a*) through a homogenous nucleation process [20]. The mixture produced remarkable brick red precipitation in the celadon solution. The Cu_2O crystal formed irregular convex, some octahedral Cu_2O crystals generated when the reaction time reached 30 min (Fig. 7*b*). Further, the colour became dirty red. According to the theory of Ostwald ripening [21, 22], small crystals would dissolve and redeposit onto larger crystals. When the reaction proceeded for 1 h, the convex in Fig. 7*b* (see arrows) gradually dissolved. Some were used as raw materials for the growth of octahedral Cu_2O crystal, while others remained in the solution. The particles became shrinkage and uneven octahedral Cu_2O formed with an average edge size of about 1 μm (Fig. 7*c*). Then, small particles (see Fig. 7*c*, arrows) dissolved, which were used as the raw materials for the further growth of crystal planes and crystal edges of the larger crystals. Finally, when the reaction lasted for 2 h, the colour of solution became brick red and the Cu_2O crystallite was regular truncated octahedral (Fig. 7*d*). If the reaction time was prolonged, the morphology of Cu_2O greatly changed because many Cu_2O crystallites reunited with each other and large-irregular agglomerates formed. According to the experiment, we proposed a possible formation mechanism of truncated octahedral Cu_2O (Fig. 8). At the beginning of the reaction, the spherical Cu_2O particle nucleated. As the reaction proceeded, the polyhedral particles grew along different directions with different growth rates due to their different surface

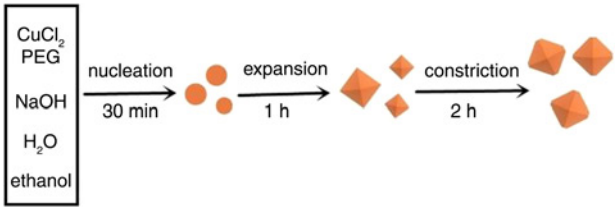

Fig. 8 *Growth mechanism of the truncated octahedral Cu_2O*

doi: 10.1049/mnl.2015.0512

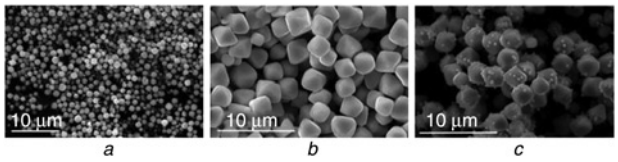

Fig. 9 *SEM images of products with the different temperature*
a 0°C
b 25°C
c 60°C

energies. As $\gamma\{111\} < \gamma\{200\} < \gamma\{110\}$.{111} planes have lowest growth rate due to the lowest surface energy. The growth of crystal is perpendicular to this plane, resulting in a change in the final morphology. Hence {111} and {200} faces can be easily maintained in the final appearance and the crystal developed into truncated octahedral structure [23].

The influence of reaction temperature on the formation of Cu_2O particles was also investigated at 0°C, 25°C and 60°C. When the temperature decreased to 0°C, the SEM image showed that the Cu_2O particles were spheroidal with non-uniform size (Fig. 9*a*). As was shown in Fig. 9*b*, the uniform and dispersive truncated octahedral Cu_2O formed at 25°C. When the reaction system was kept at 60°C (Fig. 9*c*), different shapes of Cu_2O crystal formed due to recrystallisation. The variation of supersaturation and undercooling caused by temperature change will alter the specific surface energies and relative growth rates of different planes, leading to the formation of different morphologies [24]. Such results further verified the mechanism we proposed in the previous part of this work for the growth of the truncated octahedral Cu_2O crystallites. In addition, the growth process of crystallites is a kinetically and thermodynamically controlled process that can form different shapes through changes in the reaction parameters [25].

The biomedical properties of Cu_2O were studied by exploring antibacterial property of as-prepared sample. This study was performed according to the microdilution test and it provided results of the growth inhibition of certain microorganism. The Cu_2O solutions strongly inhibited the growth of both gram positive and gram negative bacteria. The bacteria were inoculated into Cu_2O solutions with different concentrations and incubated at 37°C for 16 h. The antibacterial activity of truncated octahedral Cu_2O was evaluated by an ELISA. The percentage of bacterial growth inhibition was calculated as indicated earlier (Banjara *et al*. 2012) as follows: percentage of growth inhibition = (OD of control –OD of test)/OD of control × 100% (OD means optical density). The Cu_2O solutions were diluted to concentrations of 400, 200, 100 and 50 ug ml^{-1} by culture medium. Fig. 10 presented the antibacterial activity as a function of different concentrations of Cu_2O solutions. It can be clearly seen that Cu_2O inhibited the growth of *S. aureus* to 33.33% and *E. coli* to 24.15% at concentration of 50 μg ml^{-1}. The Cu_2O solution with the concentration of 400 μg ml^{-1} exhibited strong antibacterial efficiency of *S. aureus* to 94.76% and *E. coli* to 90.01%. The antibacterial activity of the synthesised Cu_2O varied along with the bacterial species and concentrations of Cu_2O.

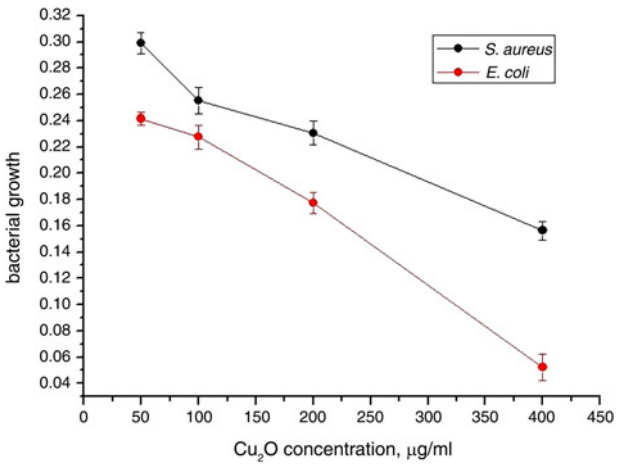

Fig. 10 *Antibacterial activity of truncated octahedral Cu_2O at various concentrations towards*

The growth inhibition percentage of ZnO on *S. aureus* and *E. coli* was 92.5%, 88% at the concentration of 400 μg ml^{-1}, respectively [26]. Obviously, truncated octahedral Cu_2O prepared in this work had more effective antibacterial activity. In addition, compared with cubic Cu_2O, the as prepared truncated octahedral Cu_2O crystals had a high selectivity for these bacteria [27]. As we all know, living issue of fungi, bacteria and viruses contain proteins. At first, Cu_2O particles were absorbed on the outside of cells. Then Cu_2O particles were penetrated into the recombinant protein on cell membrane, and reacted with the protease. The cell wall was decomposed and the interior of the cell was infected, indicating that the outer membrane of the cell was damaged, leading to the interior component [28]. Therefore, the as prepared Cu_2O crystals showed extremely potential in the biomedical engineering field, which could be applicable to medical devices.

4. Conclusion: In this paper, the truncated octahedral Cu_2O with an average size of 2.5 μm and good dispersity have been prepared by an environment friendly, low energy consumption and convenient method. It is found that the parameters of time, temperature and polyethylene glycol influence the formation of cuprous oxide. The formation mechanism of truncated octahedral Cu_2O is proposed. The prepared Cu_2O shows strong antibacterial activity towards both Gram-negative and Gram-positive bacteria. The inhibition ratio of *S. aureus* is close to 94.76% and that of *E. coli* approaches to 90.01% when the concentration of Cu_2O is 400 μg ml^{-1}. It indicates that truncated octahedral Cu_2O can be a potential fungicide, which is widely applied in biomedical, disease prevention and sensing. Taking cost and approach into consideration, the truncated octahedral Cu_2O have more advantages over the existing ones for environmental remediation. In addition, the truncated octahedral-mediated approach can be applied to synthesise other truncated octahedral inorganic materials.

5. Acknowledgments: This work was supported by the Chongqing Key Natural Science Foundation (cstc2012jjB50011), the Fundamental Research Key Funds for the Central Universities (XDJK2013B017, XDJK2016C003), and Chongqing Fundamental and Advanced Science Research Projects (cstc2013jcyjA50015). We would like to thank Prof Xiaoyu Xu from the College of Pharmaceutical Sciences for her helping with the bacteriostasis experiments.

6 References

[1] Wang Y., Zheng Y., Huang C., *ET AL.*: *Am. Chem. Soc.*, 2013, **135**, pp. 1941
[2] Su X., Chang J., Wu S., *ET AL.*: 'Synthesis of highly uniform Cu_2O spheres by a tow step approach and their assembly to form photonic crystals with a brilliant color', *J. R. Soc. Chem.*, 2016, **8**, pp. 6155–6161
[3] Park T., Papaefthymiou G.C., Viescas A.J., *ET AL.*: 'Size-dependent magnetic properties of single-crystalline multiferroic $BiFeO_3$ nanoparticles', *J. Nano Lett.*, 2007, **3**, pp. 766–772
[4] Raimondi F., Scherer G.G., Kötz R., *ET AL.*: 'Nanoparticles in energy technology: Examples from electrochemistry and catalysis', *J. Angew. Chem. Int. Ed.*, 2005, **44**, pp. 2190–2209
[5] Tian J.Q., Li H.Y., Xing Z.C., *ET AL.*: 'One-pot green hydrothermal synthesis of CuO-Cu_2O-Cu nanorod decorated reduced graphene oxide composites and their application in photocurrent generation', *J. Cstal. Sci. Technol.*, 2012, **2**, pp. 2227–2230

[6] Tsai C.H., Fei P.H., Chen C.H.: 'Investigation of coral-like Cu_2O Nano/microstructures as counter electrodes for dye-sensitized solar cells', *J. Mater.*, 2015, **8**, pp. 5715–5729
[7] Zheng Z.K., Huang B.B., Wang Z.Y., *ET AL.*: 'Crystal faces of Cu_2O and their stabilities in photocatalytic reactions', *J. Phys. Chem. C.*, 2009, **113**, pp. 14448–14453
[8] Pang H., Gao F., Lu Q.Y.: 'Morphology effect on antibacterial activity of cuprous oxide', *J. Chem. Commun.*, 2009, **9**, pp. 1076–1078
[9] Deng S., *ET AL.*: 'Reduced graphene oxide conjugated Cu_2O nanowire mesocrystals for high-performance NO_2 gas sensor', *J. Am. Chem. Soc.*, 2012, **134**, pp. 4905–4917
[10] Kang W.P., Liu F.L., Su Y.L., *ET AL.*: '*J. Cryst. Eng. Commun.*', 2011, **13**, pp. 4174
[11] Hung L.I., Tsung C.K., Huang W.Y., *ET AL.*: 'Room-temperature formation of hollow Cu2O nanoparticles', *J. Adv. Mater.*, 2010, **22**, pp. 1910–1914
[12] Yermakov A.Y., Uimin M.A., Mysik A.A., *ET AL.*: 'Magnetism and optical properties of nanocrystalline Cu_2O and TiO_2 powders', *J. Exp. Theor. Phys.*, 2007, **1**, pp. 65–68
[13] Xu H.L., Wang W.Z., Zhu W.: 'Shape evolution and size-controllable synthesis of Cu_2O octahedra and their morphology-dependent photocatalytic properties', *J. Phys. Chem. B.*, 2006, **110**, pp. 13829–13834
[14] Kuo C.H., Chen C.H., Huang M.H.: '*J. Adv. Funct. Mater.*', 2007, **17**, pp. 3773–3780
[15] Yue Y.M., Chen M.J., Ju Y.J.: 'Control of the diameters of Cu_2O nanowires fabricated by the thermal stress-induced method', *Nanosci. Nanotechnol. Lett.*, 2012, **4**, pp. 414–419
[16] Liang X.D., Gao L., Yang S.W.: 'Facile synthesis and shape evolution of single-crystal cuprous oxide', *J. Adv. Mater.*, 2009, **21**, pp. 2068–2071
[17] Xu J.S., Xue D.F.: ' Five branching growth patterns in the cubic crystal system: A direct observation of cuprous oxide microcrystals', *J. Acta Mater.*, 2007, **55**, pp. 2397–2406
[18] Lu C.H., *ET AL.*: 'One-pot synthesis of octahedral Cu_2O nanocages via a catalytic solution route', *J. Adv. Mater.*, 2005, **17**, pp. 2562–2567
[19] Roosen A.R., Carter W.C.: 'Simulations of microstructural evolution: anisotropic growth and coarsening', *J. Physica A.*, 1998, **261**, pp. 232–247
[20] Zheng H.Y., Qin L.Z., Lin H., *ET AL.*: 'Convenient route to well-dispersed Cu_2O nanospheres and their use as photocatalysts', *J. Nanosc. Nanotechnol.*, 2015, **15**, pp. 1–6
[21] Wang Y.H., Chen P.L., Liu M.H.: 'Synthesis of well-defined copper nanocubes by a one-pot solution process', *J. Nanotechnol.*, 2006, **17**, pp. 6000–6006
[22] Ostwald W.: 'Studies on the formation and transformation of solid bodies', *Zeitschrift für physikalische Chemie.*, 1897, **22**, pp. 289–330
[23] Sui Y.M., Fu W.Y., Yang H.B.: 'Low temperature synthesis of Cu_2O crystals: shape evolution and growth mechanism', *J. Crystal Growth Des.*, 2010, **11**, pp. 99–108
[24] Li C.C., Cai W.P., Cao B.Q., *ET AL.*: 'Mass synthesis of large, single-crystal Au nanosheets based on a polyol process', *J. Adv. Funct. Mater.*, 2006, **16**, pp. 83–90
[25] Quan Z.W., Li C.X., Zhang X.M., *ET AL.*: 'Two-dimensional β-NaLuF4 hexagonal microplates', *J. Crystal Growth Des.*, 2008, **8**, pp. 923–929
[26] Padmavathy N., Vijayaraghavan R.: 'Enhanced bioactivity of ZnO nanoparticles-an antimicrobial study', *J. Sci. Technol. Adv. Mater.*, 2008, **9**, pp. 1–7
[27] Pang H., Gao F., Lu Q.: 'Morphology effect on antibacterial activity of cuprous oxide', *J. Chem. Commum.*, 2009, **9**, pp. 1076–1078
[28] Hu C., Guo J., Qu J.H., *ET AL.*: 'Efficient destruction of bacteria with Ti(IV) and antibacterial ions in co-substituted hydroxyapatite films', *J. Appl. Catal. B Environ.*, 2007, **73**, pp. 345–353

doi: 10.1049/mnl.2015.0512